Immunoreactivity of Humanized Single-Chain Variable Fragment Against Its Functional Epitope On Domain 1 of CD147

Nutjeera Intasai
Chiang Mai University
Kuntalee Rangnoi
Suranaree University of Technology
Montarop Yamabhai
Suranaree University of Technology
Thanathat Pamonsupornwichit
Chiang Mai University
Suthinee Soponpong
Chiang Mai University
Weeraya Thongkum
Chiang Mai University
Umpa Yasamut
Chiang Mai University
Koollawat Chupradit
Mahidol University
Nuchira Takheaw
Chiang Mai University
Piyarat Nimmanpipug
Chiang Mai University
Chatchai Tayapiwatana (chatchai.t@cmu.ac.th)
Chiang Mai University

Research Article

Keywords: domain 1, CD147, epitope, ScFv, humanized, cancer, targeted therapy

Posted Date: October 19th, 2021

DOI: https://doi.org/10.21203/rs.3.rs-964906/v1

Immunoreactivity of humanized single-chain variable fragment against its functional epitope on domain 1 of CD147

Nutjeera Intasai[1,2,3], Kuntalee Rangnoi[4], Montarop Yamabhai[4], Thanathat Pamonsupornwichit[2,3], Suthinee Soponpong[2,3], Weeraya Thongkum[2,3,5], Umpa Yasamut[2,3,5], Koollawat Chupradit[2,6], Nuchira Takheaw[5,7], Piyarat Nimmanpipug[8], Chatchai Tayapiwatana[2,3,5*]

[1]Division of Clinical Microscopy, Department of Medical Technology, Faculty of Associated Medical Sciences, Chiang Mai University, Chiang Mai, Thailand
[2]Center of Biomolecular Therapy and Diagnostic, Faculty of Associated Medical Sciences, Chiang Mai University, Chiang Mai, Thailand,
[3]Center of Innovative Immunodiagnostic Development, Department of Medical Technology, Faculty of Associated Medical Sciences, Chiang Mai University, Chiang Mai, Thailand
[4]Molecular Biotechnology Laboratory, School of Biotechnology, Institute of Agricultural Technology, Suranaree University of Technology, Nakhon Ratchasima, Thailand
[5]Division of Clinical Immunology, Department of Medical Technology, Faculty of Associated Medical Sciences, Chiang Mai University, Chiang Mai, Thailand
[6]Siriraj Center for Regenerative Medicine, Faculty of Medicine Siriraj Hospital, Mahidol University, Bangkok, Thailand
[7]Biomedical Technology Research Center, National Center for Genetic Engineering and Biotechnology, National Science and Technology Development Agency at the Faculty of Associated Medical Sciences, Chiang Mai University, Chiang Mai, Thailand
[8]Department of Chemistry, Faculty of Science, Chiang Mai University, Chiang Mai, Thailand

ABSTRACT

Domain 1 of CD147 participates in matrix metalloproteinase (MMP) production and is a candidate for targeted therapy to prevent cancer invasion and metastasis. A functional mouse anti-CD147 monoclonal antibody, M6-1B9, was found to recognize domain 1 of CD147, and its respective mouse single-chain variable fragment (ScFvM61B9) was subsequently generated. The EDLGS epitope candidate for M6-1B9 was identified using the phage display peptide technique in this study. For future clinical applications, humanized ScFv specific to domain 1 of CD147 (HuScFvM61B9) was partially adopted from the hypervariable sequences of parental mouse ScFvM61B9 and grafted onto suitable human immunoglobulin frameworks. Molecular modelling and simulation were performed in silico to generate the conformational structure of HuScFvM61B9. These

results elucidated the amino acid residues that contributed to the interactions between CDRs and the epitope motif. The expressed HuScFvM61B9 specifically interacted with CD147 at the same epitope as the original mAb, M6-1B9, and retained immunoreactivity against CD147 in SupT1 cells. Binding affinity of HuScFvM61B9 by biolayer interferometry was higher than the predicted one. should be considered a potential therapeutic antibody. As domain 1 is responsible for cancer invasion and metastasis, HuScFvM61B9 would be a candidate for cancer targeted therapy in the future.

Keywords: domain 1, CD147, epitope, ScFv, humanized, cancer, targeted therapy

Introduction

CD147, a transmembrane glycoprotein in the immunoglobulin superfamily, is highly expressed in various cancer cell types. CD147 plays an important role in the regulation of several cancer cellular processes, including proliferation, invasion, metastasis, angiogenesis, glycolysis, and chemoresistance[1,2]. Domain 1 (IgC2 domain) of CD147 is important in matrix metalloproteinase (MMP) production, which leads to the degradation of the basement membrane and extracellular matrix and promotes tumor proliferation, invasion, and metastasis[3]. The disruption of CD147 dimerization can prevent cancer cell invasion and metastasis[4]. In comparison to the strengths of other therapeutic antibodies, immunotargeting of the CD147 functional domains is considered a promising candidate for cancer immunotherapy in preventing cancer invasion and metastasis[5-13]. A therapeutic mouse anti-CD147 monoclonal antibody (mAb), HAb18, recognizes the residue ^{39}LTCSLNDSATEV^{50} in domain 1 of CD147 and exerts an anti-metastatic activity in hepatocellular carcinoma through the reduction of MMPs[5,6].

The functional epitope of M6-1B9, a mouse anti-CD147 mAb, was formerly characterized as residing on domain 1[14,15]. Subsequently, mouse single-chain fragment variable of M6-1B9 (ScFvM61B9) was generated from the cDNA of hybridoma clone

M6-1B9 to be expressed as soluble ScFvM61B9 and ScFvM61B9 intrabody forms[16]. Soluble ScFvM61B9 inhibited T-cell proliferation after stimulation with an anti-CD3 mAb[17]. ScFvM61B9 activity has not yet been studied in solid tumors. However, the ScFvM61B9 intrabody was previously found to inhibit the cell surface expression of CD147 and decreased the aggressiveness of various cancers *via* specific mechanisms[17-21]. Although the ScFvM61B9 intrabody did not affect either MMP-2 or MMP-9 activities in the cervical cancer HeLa cell line, it suppressed urokinase-type plasminogen activator (uPA) and inhibited HeLa cell metastasis[17,20]. In addition, the ScFvM61B9 intrabody affected the α3β1-integrin and MCT-1 function and suppressed the progressive phenotype in the colorectal cancer Caco-2 cell line[18]. Moreover, the ScFvM61B9 intrabody promoted intracellular acidosis and induced apoptosis in the Caco-2 cell line[19]. Correspondingly, immunotargeting of CD147 domain 1 is feasible for cancer immunotherapy.

To verify whether the epitope recognized by M6-1B9 was unique, the phage display peptide technique was applied. Several protocols have been proposed to obtain therapeutic antibodies[22]. The complementarity-determining region (CDR)-graft-humanized antibody is comparatively cost-effective among its peers because the annotated sequences of variable domains from a candidate mouse monoclonal antibody can be directly submitted for *in situ* design. Transplanting the CDR of a murine antibody onto a human antibody framework is commonly performed to diminish the potential immunogenicity of antibodies for humans[23]. For future clinical applications, the peptide sequences of heavy and light chain frameworks of ScFvM61B9 were automatically replaced with human frameworks *via* BioLuminate analysis in this study. The T20 score analyzer[24] was then selected to quantify the humanness of humanized ScFvM61B9 (HuScFvM61B9). A BLAST search[25] of an input HuScFvM61B9 sequence was

performed against the 38,708 human antibody-variable region sequences in the reference database. The T20 score was derived from the average percent sequence identities between a HuScFvM61B9 sequence and the top 20 matched sequences. The candidate pose of HuScFvM61B9 complexing with domain 1 of CD147 was identified *via* ClusPro 2.0, relying on the knowledge base peptide sequence from the fetched phage clones. As the functions of proteins are crucially related to their molecular assembly, molecular modelling techniques used to determine binding structures have been comprehensively explored to exemplify possible complex-forming mechanisms[26,27]. An accountable design of novel antibodies together with binding in protein–protein complexes can be initialized using protein docking[28,29]. A predicted HuScFvM61B9-CD147 binding structure from the Schrödinger BioLuminate module was characterized in this study[30]. The binding affinity of HuScFvM61B9 was determined using biolayer interferometry. Subsequently, the immunoreactivity of the generated HuScFvM61B9 was compared against the parental M6-1B9 mAb and other mAbs against CD147. To ascertain HuScFvM61B9 immunoreactivity, the inhibitory binding of HuScFvM61B9 to CD147Rg with anti-CD147 mAbs was analyzed. The immunofluorescence reactivity of HuScFvM61B9 against CD147 on the cell surface of SupT1 cells was determined *via* flow cytometry to acquire information necessary for biological function assays.

Results

Identification of M6-1B9 monoclonal antibody epitope through biopanning of phage display combinatorial peptide library

After three rounds of bio-panning, 16 phage clones were randomly chosen to identify the bona fide binding partner to M6-1B9 mAb *via* phage enzyme-linked immunosorbent assay (ELISA) (Figure 1a). Fourteen clones that showed specific binding to M6-1B9 mAb were selected to determine the DNA and amino acid sequences. One phage clone (11)

showed no peptide sequences. The deduced peptide sequences are presented in Figure 1b. Among them, three clones (10, 12, and 14) shared the EDxGS motif (x is any amino acid residue). The specific binding activity of these clones to M6-1B9 mAb was confirmed again with an isotype control by ELISA, as shown in Figure 1c. Phages 10, 12, and 14 were able to bind specifically to M6-1B9 mAb but not to the anti-P24 and anti-IFN-γ mAbs. The amino acid sequences of these three clones were aligned with the human CD147 sequence using Clustal Omega. Alignment revealed that all three clones shared less than three continuous amino acid residues identical to the sequence of human CD147 registered in GenBank, which indicated that these peptides were likely the mimotope of CD147 (Figure 1d). Because the EDLGS motif is not present in mouse CD147, the retrieved phage peptide demonstrates a strong tendency to be an antigenic determinant.

a

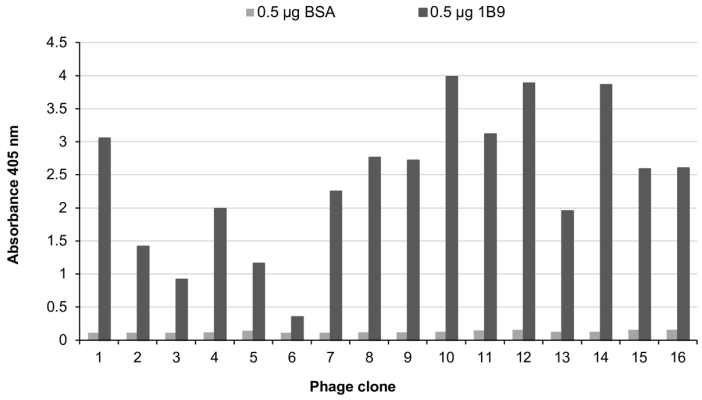

b

Phage clone	Amino acid sequence
1	GGTSGYFNPENE
2	TQSGNVVSPLVF
4	VDTGRGWAEITS
5	MHAWAVPGGGQV
7	AGGSQVKTRHSE
8	MVGGQGVWEGDG
9	GGGALPNEPLTH
10	KR**ED**C**GS**SWCRE
12	LSS**ED**L**G**VG**S**LF
14	T**ED**C**G**AS**S**CAMA
13	HAGAQGGWVADS
15	VARMDSLQDRDN
16	KGLPRQTMAPAA

c

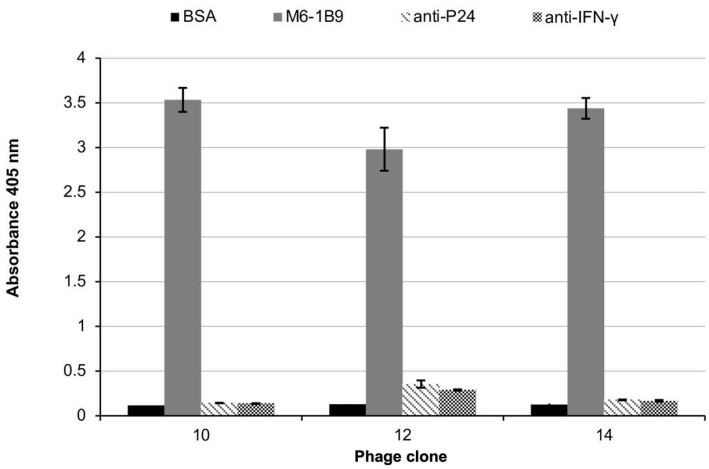

d

Figure 1. Binding of phage clones to M6-1B9 mAb and the predict motif, EDxGS. (**a**) Binding activity of selected phage clones to M6-1B9 mAb *via* phage peptide ELISA. The ELISA wells were coated with 0.5 µg of M6-1B9 mAb and 0.5 µg BSA as a negative control. Bound phage was detected with an HRP-conjugated anti-M13 antibody. The absorbance at 405 nm was measured using a microtiter plate reader. (**b**) Amino acid sequences of the 12-mer peptides from selected phage clones. The amino acids of each CDR interacting with the epitope on domain 1 of CD147 are depicted in red letters. (**c**) Confirmation of binding activity of positive phage peptides *via* ELISA. Three identified mimotope peptides possessing a consensus motif were tested for the binding against M6-1B9, anti-P24, and anti-IFN γ mAbs. A bound phage was detected with an HRP-conjugated anti-M13 antibody. Triplicate measurements of absorbance values at 405 nm with standard deviations were reported. (**d**) Amino acid sequence alignment of selected phage clones and human CD147. The predict motif EDxGS is shown in red letters, and is correlated to the amino acid on CD147 (bold). The CD147 human sequence is from GeneBank (AB085790.1).

Humanization of mouse ScFvM61B9

The original peptide sequences of the heavy and light chain frameworks of mScFvM61B9 were automatically substituted with human frameworks *via* BioLuminate analysis. The alignment of the amino acid sequences of parental ScFvM61B9 versus HuScFvM61B9 is shown in Figure 2. The T20 humanness score improved from 92.3 to 100.05 and 60.9 to 82.54 for heavy and light chains, respectively. The human germlines of HuScFvM61B9 are IGHV3 and IGKV1.

```
mH_M61B9    1   EVKLLESGGGLVKPGGSLKLSCAASGFTFSSYAMSWVRQTPEKRLEWVATISSGGTYTYYPDSVKGRFTISRDNAKNTLYLQMSSLRSED 90
                EV+L+ESGGGLV+PGGSL+LSCAASGFTFSSYAMSWVRQ P K LEWVATISSGGTYTYYPDSVKGRFTISRDN+KNTLYLQM+SLR+ED
hH_M61B9    1   EVQLVESGGGLVQPGGSLRLSCAASGFTFSSYAMSWVRQAPGKGLEWVATISSGGTYTYYPDSVKGRFTISRDNSKNTLYLQMNSLRAED 90

mH_M61B9    91  TAMYYCARFRNGAYWGQGTLVTVSA 115
                TA+YYCARFRNGAYWGQGTLVTVS+
hH_M61B9    91  TAVYYCARFRNGAYWGQGTLVTVSS 115

mL_M61B9    2   MTQTPALMAASPGEKVTITCSVSSSISSSNLHWYQQKSETSPKPWIYGTSNLASGVPVRFSGSGSGTSYSLTISSMEAEDAATYYCQQWS 91
                MTQ+P+ ++AS G++VTITCSVSSSISSSNLHWYQQK   +PKPWIYGTSNLASGVP RFSGSGSGT Y+LTISS++ ED ATYYCQQWS
hL_M61B9    4   MTQSPSSLSASVGDRVTITCSVSSSISSSNLHWYQQKPGKAPKPWIYGTSNLASGVPSRFSGSGSGTDYTLTISSLQPEDFATYYCQQWS 93

mL_M61B9    92  NYPLTFGAGTKLELK 106
                NYPLTFG GTK+E+K
hL_M61B9    94  NYPLTFGQGTKVEIK 108
```

Figure 2. Alignment result of mouse ScFvM61B9 (mL and mH) against HuScFvM61B9 (hL and hH).

Molecular model of HuScFvM61B9 against CD147 domain 1

Ten candidate complexes were obtained from the ClusPro 2.0 Web server. The interactive residues on the predicted complexes were analyzed using the Prodigy Web server[31]. The most likely pose illustrating the interactive epitope residues correlating with the amino acid sequence identified using the phage-display peptide was verified (Figure 3a). Pymol software was used to visualize the residues found on the contact surface using the Pymol code generated from Prodigy (Figure 3b).

Amino acid residue contributions and interaction types were examined to understand the intermolecular interactions that can improve discovery. From the selected candidate, we estimated a possible intermolecular residue interaction based on the atomic coordinates. We identified hydrogen bonds of the D-H…A type (donor atom D and acceptor atom A)

using the following distance and angle criteria: d(D…A) ≤ 3.5 Å, θ(D-H…A) ≥ 90°. Atom-π, π-π, and hydrophobic *van der Waals* interactions were analyzed using the centroid−centroid and between heavy atoms criteria with a maximum distance of 6.0 Å.

a

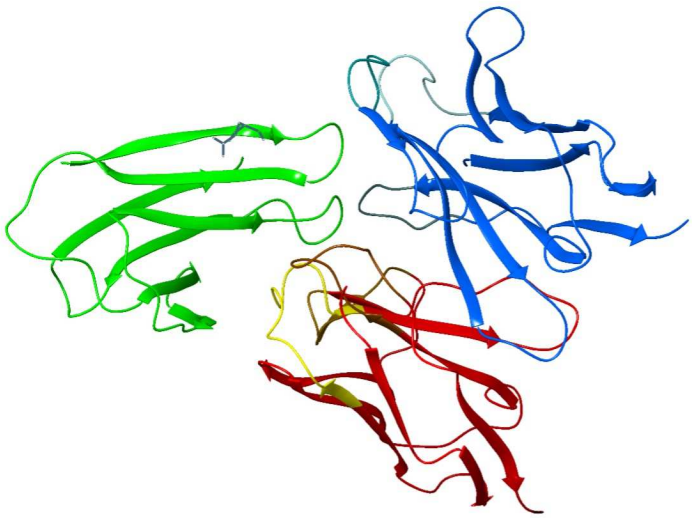

b

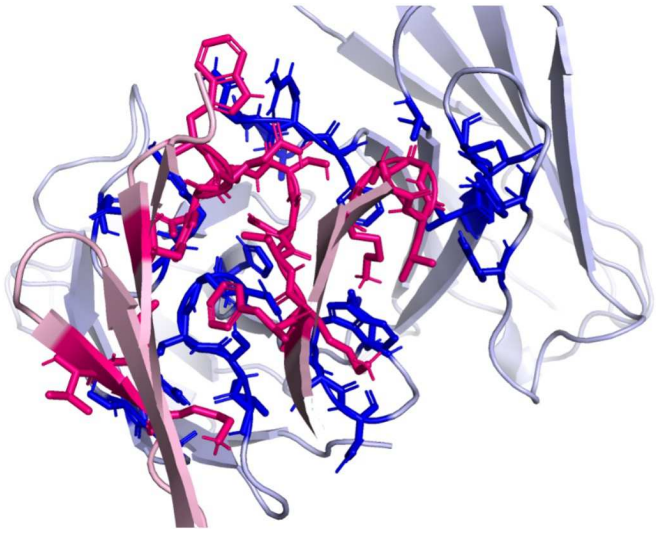

Figure 3. Model and amino acid residues participating of interaction of HuScFvM61B9 against domain 1 of CD147. (**a**) Automatic masking of non-CDR

regions of the antibody mode in ClusPro 2.0 is applied to predict the interaction coordinate of HuScFvM61B9 against domain 1 of CD147 conformational structures generated from BioLuminate 4.0. The H-chain and L-chain variable domains are shown as blue and red ribbons, respectively. The domain 1 target is depicted as a green ribbon. (**b**) The Prodigy Web server was used to elucidate the molecular interaction of the selected complex from the ClusPro 2.0 output. Based on the Pymol code automatically generated by Prodigy, the crucial side-chain residues on CDRs of HuScFvM61B9 and domain 1 (consisting of the EDLGS epitope) at the binding interface are labeled in blue and red, respectively. The predicted binding affinity (K_D) is 1.60×10^{-8}.

Analysis of generated HuScFvM61B9 structure

The original mScFvM61B9 and the predicted HuScFvM61B9 structures using BioLuminate were compared (Figure 4a). The analyzed root-mean-square deviation (RMSD) was 0.758 Å. The CDRs of HuScFvM61B9 were identified using PyIgClassify on the HScFvM61B9 structure (Figure 4b). The most likely complex of HuScFvM61B9 and domain 1 of CD147 was selected from ClusPro 2.0 based on the epitope; that is, EDLGS was retrieved from the phage peptide analysis. The molecular interaction of HuScFvM61B9 against the epitope residing in domain 1 of CD147 was analyzed using Prodigy.

a

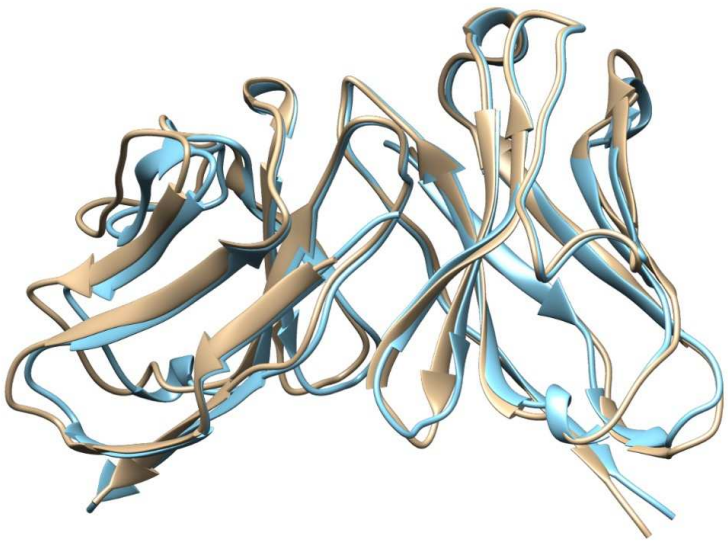

b

Chain	Sequence	Residue Numbers	CDR	Cluster
L	DIQMTQSPSSLSASVGDRVTITC	[1 - 23]	frame	-
L	SVSSSISS**SN**L**H**	[24 - 34]	L1	L1-12-1
L	WYQQKPGKAPKPWI	[35 - 48]	frame	-
L	**Y**GTSNLAS	[49 - 56]	L2	L2-8-1
L	GVPSRFSGSGSGTDYTLTISSLQPEDFATYYC	[57 - 88]	frame	-
L	**QQW**SN**Y**P**L**T	[89 - 97]	L3	L3-9-cis7-1
L	FGQGTKVEIKR	[98 - 108]	frame	-
H	EVQLVESGGGLVQPGGSLRLSC	[1 - 22]	frame	-
H	AASGFTFS**SYAMS**	[23 - 35]	H1	H1-13-1
H	WVRQAPGKGLEWVA	[36 - 49]	frame	-
H	**TISSGGTY**T**Y**	[50 - 58]	H2	H2-10-2
H	YPDSVKGRFTISRDNSKNTLYLQMNSLRAEDTAVYYC	[59 - 92]	frame	-
H	AR**FRN**GAY	[93 - 102]	H3	H3-8-1
H	WGQGTLVTVSS	[103 - 113]	frame	-

Figure 4. Structural comparison of parental ScFvM61B9 (gold ribbon) versus HuScFvM61B9 (blue ribbon) and identification and clustering of HuScFvM61B9 CDRs. The conformational structures were obtained from the BioLuminate 4.0 antibody humanization process. The calculated RMSD between 108 pruned atom pairs is 0.758 Å (across all 115 pairs: 1.004) as per the MatchMaker function in the UCSF Chimera 1.15 software with the Needleman-Wunsch algorithm/BLOSUM-62. (**b**) The amino acids of each CDR interacting with the epitope on domain 1 of CD147 are depicted in red letters.

Atomic-level intermolecular interactions in the HuScFvM61B9-CD147 binding structure

This atomistic picture of the structural assembly was in accordance with the epitope mapping analysis results. The structure of the complex suggested that hydrogen bonding and *van der Waals* interactions are key in this protein-protein association. The crucial side-chain residues on CDRs of HuScFvM61B9 and domain 1 (composed of EDLGS epitope) at the binding surface are labeled in Figure 5. From the complex, S52, Y56, and Y58 in HuScFvM61B9 CDR H2 formed hydrogen bonds with domain 1 of CD147. For HuScFvM61B9, CDR H1, H3, A33, and F95 interacted with domain 1 of CD147 at a longer distance *via van der Waals* interactions.

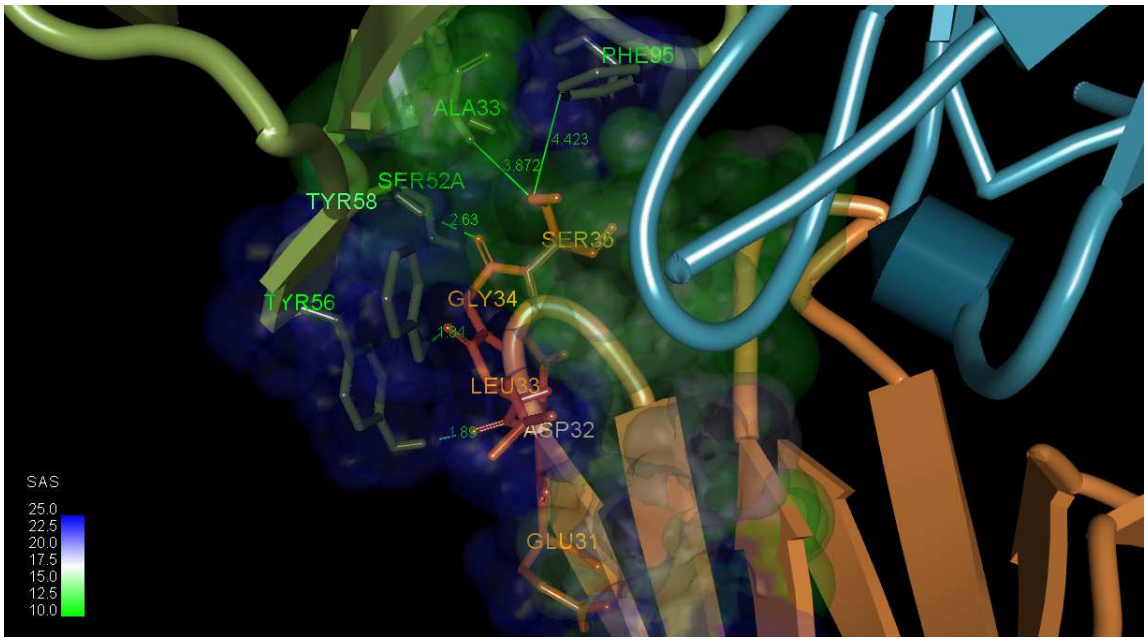

Figure 5. Atomic-level observation of amino acid residues participating in the HuScFvM61B9-CD147 predicted binding structure. Key residues on CDRs of HuScFvM61B9 and domain 1 of CD147 at the binding surface are highlighted in green and orange, respectively.

Expression of recombinant protein HuScFvM61B9

The HuScFvM61B9 protein was expressed in *Escherichia coli* (*E. coli*) Origami B (DE3) and purified *via* affinity chromatography. The results revealed that the purified HuScFvM61B9 protein containing a His6x tag was successfully produced. The recombinant protein at approximately 26 kDa was detected *via* SDS-PAGE (Figure 6a) and Western immunoblotting (Figure 6b).

a

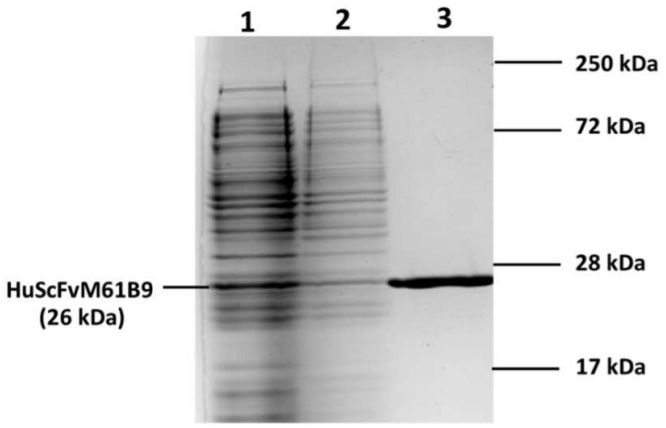

b

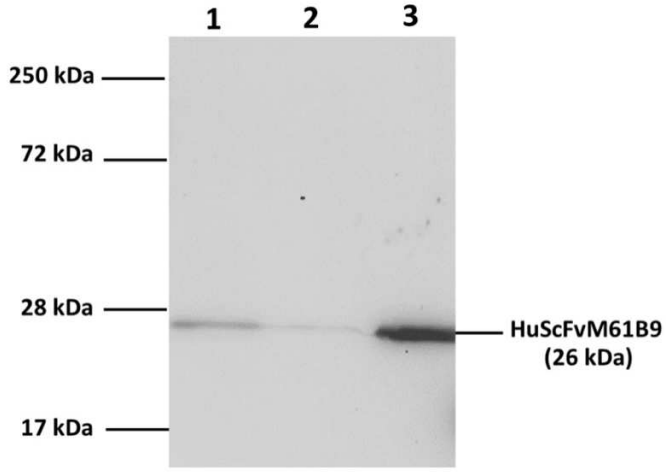

Figure 6. Detection of purified HuScFvM61B9 *via* SDS-PAGE and Western blot analysis. (**a**) The crude proteins extracted from bacteria and the purified recombinant protein were subjected to 15% SDS-PAGE analysis. Crude lysate proteins (lane 1), crude pellet proteins (lane 2), and purified HuScFvM61B9 (lane 3) are shown. The protein bands were visualized through PAGE Blue staining. (**b**) Proteins were separated by SDS-PAGE, transferred onto a PVDF membrane, and subsequently probed with an HRP-conjugated anti-His-tag antibody (dilution 1:3000). The reaction was developed using a chemiluminescent substrate detection system. Crude lysate proteins (lane 1), crude pellet proteins (lane 2), and purified HuScFvM61B9 (lane 3) are shown.

Binding affinity of HuScFvM61B9

The results demonstrated that HuScFvM61B9 successfully bound to its target, CD147,

which was immobilized on the Protein G biosensor tip at 30 °C. The binding affinity (K_D), at $4.87 \pm 1.24 \times 10^{-9}$ (mean ± SD), was assessed based on the association and dissociation constants using the Octet K2 system.

Determination of HuScFvM61B9 binding activity

The binding activity of the purified HuScFvM61B9 to CD147 was investigated. The OD values at 450 nm were increased in concentration-dependent manner (Figure 7a). This result suggested that purified HuScFvM61B9 was successfully bound to its target, CD147.

Inhibition binding analysis of HuScFvM61B9 and anti-CD147 mAbs

Inhibition binding activity was determined using inhibition ELISA. The mouse anti-CD147 mAbs (M6-1B9 and M6-1E9) inhibited the binding of purified HuScFvM61B9 to immobilized CD147Rg in a concentration-dependent manner (Figure 7b). These data demonstrated that HuScFvM61B9, M6-1B9, and M6-1E9 were bound to CD147 at the same or contiguous epitope.

Reactivity of HuScFvM61B9 to CD147 on SupT1 cells

Flow cytometric analysis was performed to evaluate the functional activity of HuScFvM61B9 against CD147 on SupT1 cells. The HuScFvM61B9 was strongly bound to CD147 on the cell surface of SupT1 (Figure 7c), comparable to that with its parental M6-1B9 mAb (Figure 7d). However, the relative fluorescence index of HuScFvM61B9 and M6-1B9 mAb was 40 and 99, respectively.

a

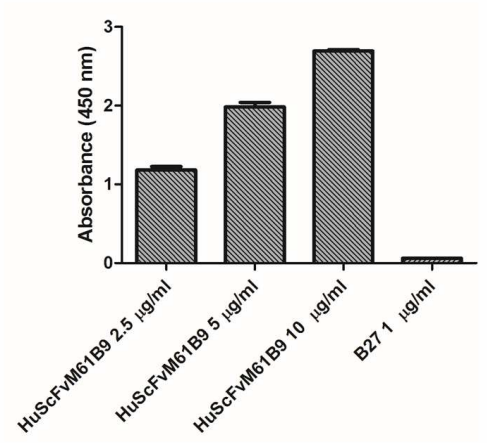

b

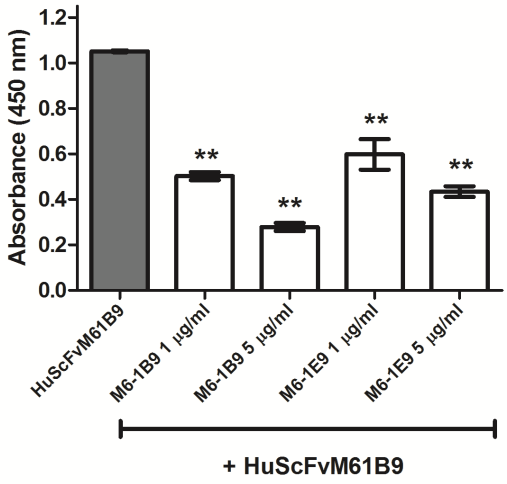

c d

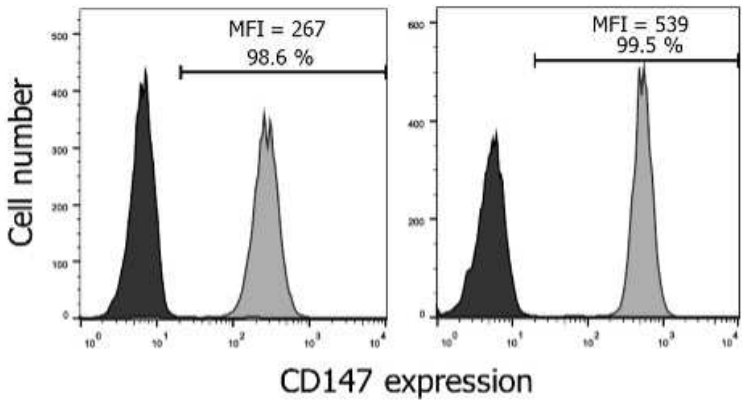

Figure 7. Immunoreactivity of HuScFvM61B9. (**a**) The microtiter plates were coated with CD147Rg, and HuScFvM61B9 was subsequently added at various concentrations to analyze the binding activity of HuScFvM61B9. HuScFvM61B9 was detected by HRP-

conjugated anti-His-tag mAb. B27 was used as an irrelevant antibody control. (**b**) The ELISA wells were coated with CD147Rg, and mouse anti-CD147 mAbs were used to inhibit the binding of HuScFvM61B9 to the target. The signal was determined using HRP-conjugated anti-His-tag mAb, and the absorbance was measured using a microtiter plate reader. The data illustrate triplicate experiments and an error bar (mean ± SD), analyzed by a paired t-test (** $p < 0.01$). Immunofluorescence analysis of the reactivity of HuScFvM61B9 (**c**) and (**d**) to CD147 on SupT1 cells. PE-conjugated anti-His tag antibody or Alexa Fluor 568 conjugated goat-anti-mouse IgG (H+L) was used as secondary antibodies, respectively. The percentage of positive cells is presented below the mean fluorescence intensity (MFI) value.

Discussion

The T20 humanness scores for the heavy and light chains of HuScFvM61B9 increased over those of the parental sequence. As a weak correlation between the T20 score of 65 therapeutic antibodies and their available immunogenicity data[24], our data suggested that the immunogenicity of HuScFvM61B9 was reduced and could potentially decrease the chance of HuScFvM61B9 immunogenicity in humans. Using the T20 humanness score, complicated and time-consuming *in vitro* experiments for immunogenicity prediction of HuScFvM61B9 were not required[24].

Phage display combinatorial peptide libraries have been successfully and efficiently used to identify a wide variety of epitopes and mimotopes from a wide variety of mAbs[32,33]. Although a linear epitope can be mapped directly to the target protein, it must be combined with computer modelling to identify binding sites on the natural target. The amino acid sequences of phage clones 10, 12, and 14 were aligned with the human CD147 sequence and shared less than three continuous amino acid residues identical to the human CD147 sequence registered in GenBank. This indicated that these peptides were likely the mimotope of CD147. The EDLGS motif was an antigenic determinant, as it was not present in mouse CD147. These data suggested that M61B9 mAb recognized the epitope

different from other anti-CD147 mAbs, including HAb18, which is used as a therapeutic antibody in hepatocellular carcinoma[5,6]. In addition, the M6-1B9 mAb recognized the EDLGS, which resides in the residues ^{22}AAGTVFTTV*EDLGS*KILLTCSLNDSATEV^{50} in domain 1 of CD147; these residues have been suggested to play a critical role in MMP secretion and tumor invasion[6]. Furthermore, the complex structure predicted by the ClusPro docking algorithm provided crucial residues for the antigen-antibody at the binding site. The analyzed RMSD was 0.758; by comparison, the Å values of mScFvM61B9 and HuScFvM61B9 indicated a similar conformation between these two ScFvs. Interestingly, the predicted complex from ClusPro was similar to the structural coordinate generated by the Rosetta SnugDock protocol (data not shown). The amino acids of each HuScFvM61B9 CDR interacting with the epitope on domain 1 of CD147 are listed in Figure 1b. This is because domain 1 of CD147 is crucial for MMP production, which leads to the degradation of the basement membrane and extracellular matrix and results in promoting of tumor proliferation, invasion, and metastasis[3]. Taken together, HuScFvM61B9 would possess the necessary functional activities, including the ability to reduce MMPs, needed to ensure a feasible targeted cancer immunotherapy regime.

When humanized ScFv is generated, the preservation of its affinity and biological function must be considered. The binding affinity of HuScFvM61B9 was 30-fold higher than that predicted by the Prodigy Web server. This result indicates that the relevance of the conformational structure of HuScFvM61B9 can be related to its binding affinity. A single amino acid substitution in the binding pocket can dramatically change the protein binding affinity of various proteins[34,35]. Considering the biological function of HuScFvM61B9, the immunoreactivity of HuScFvM61B9 revealed that HuScFvM61B9 could specifically bind to CD147 at the same epitope as its parental mAb, M6-1B9. In addition to M6-1B9, M6-1E9 also inhibited HuScFvM61B9 from binding to its target

because M6-1B9 and M6-1E9 bind to the same or contiguous epitope in domain 1 of CD147[15,36]. Moreover, HuScFvM61B9 also bound to a leukemic cell line, SupT1, with a low relative fluorescence intensity. This may be a result of the lower avidity of HuScFvM61B9 in comparison to M6-1B9 mAb. Taken together, these results imply that a humanized ScFv targeting domain 1 of human CD147 (HuScFvM61B9) was successfully constructed and retained its immunoreactivity; however, its avidity was lower than that of its parental mAb, M6-1B9. The development of HuScFvM61B9-Fc fusion (HuScFvFcM61B9) or fully humanized M61B9 IgG will be attempted in future research to solve the problem of monovalent ScFv as HER2-targeted therapy[37].

Materials and Methods

Epitope mapping *via* phage display random peptide library

Bio-panning of a 12-mer phage display random peptide library (SUT12) against the anti-CD147 mAb (clone M6-1B9) was performed as noted in previous research[32,38]. Briefly, three rounds of biopanning were performed by gradually reducing the amount of the M6-1B9 antibody, ranging from 10 to 5 and 2 μg for each consecutive round of affinity selection. After three rounds of biopanning, 16 individual phage clones were randomly chosen and amplified to assess their binding activity against the M6-1B9 mAb by phage ELISA, as previously reported[39]. The phagemid DNA from positive phage clones was prepared for nucleotide sequencing through automated DNA sequencing services using the -96gII primer (5′-CCC TCA TAG TTA GCG TAA CG-3′). The amino acid sequences were analyzed using SnapGene software.

Humanization of ScFvM61B9 and property validation

The suitable frameworks in the variable domain of HuScFvM61B9 were assigned from parental ScFvM61B9 using the antibody humanization process of the BioLuminate 4.0

demo software (Schrödinger, LLC, USA)[16]. Upon submitting the amino acid sequence of ScFvM61B9 heavy and light chain variable domains, a PDB number 6N4Q crystal structure containing a mouse Fab template was selected for conforming the possible structure. Subsequently, the human frameworks of PDB number 5HYS were automatically retrieved to substitute the frameworks of the modelled ScFvM61B9 structure to retain the canonical shape of antibody CDR loops. The structure comparison and RMSD calculation of the designed HuScFvM61B9 versus parental ScFvM61B9 were performed using UCSF Chimera 1.15 software. The CDR regions of the generated HuScFvM61B9 structure were deduced using the PyIgClassify Web server[40]. The humanness of HuScFvM61B9 was calculated using the T20 score analyzer tool[24].

Molecular model of HuScFvM61B9 against CD147 domain 1

The generated structure of HuScFvM61B9 from BioLuminate was submitted to the ClusPro 2.0 Web server along with the CD147 domain 1 extracted from PDB number 5X0T[28]. The antibody mode option was selected to automatically mask non-CDR regions in this *in silico* protein-protein docking process.

Construction of plasmid expressing HuScFvM61B9

The amino acid sequence of modified ScFvM61B9 was reverse transcribed and optimized using the GenScript web service for proper expression in *E. coli*. The *HuScFvM61B9* coding sequence containing 5′ *Nhe*I and 3′ *Hind*III restriction sites was synthesized (GenScript, USA). The synthesized polynucleotide was subsequently digested with *Nhe*I and *Hind*III and cloned into the *Nhe*I and *Hind*III sites of the pET-21a plasmid vector to generate the pET-21a-*HuScFvM61B9(HIS6X)* plasmid.

Expression and purification of HuScFvM61B9

The pET-21a-*HuScFvM61B9(HIS6X)* plasmid was transformed into competent *E. coli* Origami B (DE3) cells to produce humanized single-chain variable fragment of M61B9 containing a His6x tag (HuScFvM61B9). A single colony was picked and grown in a 5 ml super broth medium starter culture overnight at 37 °C. Then, the culture was inoculated into a 500 mL SB medium containing 0.05% glucose and 100 µg/mL ampicillin at 37 °C until an OD_{600} of 0.8 was reached. Protein expression was induced by adding 50 µM IPTG, and this process continued for 16-18 h at 20 °C. The induced bacteria expressing HuScFvM61B9 were washed twice with PBS and lysed *via* three sonication times of 5 min each at 0.5 cycles with 80% amplitude on ice. The lysed bacteria were subjected to freeze-thaw cycling, followed by centrifugation at 4000 g for 30 min at 4 °C. The cell lysate was collected and HuScFvM61B9 was purified *via* affinity chromatography on a HisTrap™ HP column (GE Healthcare) using ÄKTA Prime™ plus. The collected fractions were analyzed *via* SDS-PAGE on a 15% gel with PageBlue™ staining to determine the purity of the HuScFvM61B9 proteins. The collected fractions were subjected to Western blot analysis. Proteins were separated by SDS-PAGE, transferred onto a PVDF membrane, and subsequently probed with an HRP-conjugated anti-His-tag antibody (BioLegend, 652504) at 1:3000 dilution. The reaction was developed using a chemiluminescent substrate detection system.

Affinity determination of HuScFvM61B9 *via* biolayer interferometry

Biolayer interferometry was used to analyze the binding affinity of HuScFvM61B9 to CD147Rg (CD147 fused with human IgG Fc). CD147Rg was prepared from Chinese hamster ovarian (CHO) cells carrying the gene encoding the CD147 extracellular domain-human IgG Fc fusion protein (CD147Rg; contain domain 1 linked to domain 2); this material was kindly provided by Dr. Hannes Stockinger (Medical University of Vienna,

Austria)[41]. Briefly, CHO cells carrying the CD147Rg gene were cultured in CHO-S-SFM II medium (Gibco) with 5 mM methotrexate at 37 °C and 5% CO_2. The culture supernatant containing CD147Rg was collected and subjected to purification based on the human IgG-Fc part *via* affinity chromatography on a HiTrap Protein G HP column (GE Healthcare, Uppsala, Sweden). Prior to use, the purified CD147Rg was validated using the corresponding specific mAbs, as previously described[41]. To analyze the binding affinity of HuScFvM61B9 to CD147Rg, 2.5 μg/mL of CD147Rg was immobilized on Protein G biosensor tips (Sartorius FortéBio) and placed in 0.05 % Tween in PBS to generate the baseline. The biosensor tips were then placed into a sample comprising 5 μg/mL HuScFvM61B9 recombinant protein to analyze the association signal. Subsequently, the tips were placed in 0.05% Tween in PBS to dissociate the protein-protein interactions. The entire reaction was conducted at 30 °C at a flow rate of 30 μL/min. The association and dissociation constants were measured using the Octet K2 System (Sartorius FortéBio). The equilibrium constant K_D of HuScFvM61B9 was calculated from the ratio of the dissociation rate constant k_d to the association rate constant (k_d/k_a).

Binding assay of HuScFvM61B9 by indirect ELISA

To investigate the binding activity of HuScFvM61B9 to CD147, the indirect ELISA was performed. The microtiter plates were immobilized with 50 μL of 10 μg/mL CD147Rg and incubated overnight at 4 °C in a moist chamber. The other steps were performed at ambient temperature in a moist chamber. The coated wells were washed three times with a washing buffer (0.05 % Tween 20 in PBS), followed by blocking with 2 % skim milk in PBS for 1 h. After washing, purified HuScFvM61B9 protein was added at various concentrations to the wells and incubated for 1 h. After washing three times, 50 μL of HRP-conjugated anti-His-tag mAb (BioLegend, 652504) at 1:5000 dilution was added

and incubated for 1 h. The reaction was developed using a TMB substrate, and then the reaction was ceased with 1 N HCl. Absorbance at 450 nm was measured using an ELISA reader.

Inhibition binding analysis of HuScFvM61B9 with anti-CD147 mAbs *via* inhibition ELISA

Inhibition binding activity of purified HuScFvM61B9 was assessed using the inhibition ELISA. Fifty microliters of 10 μg/mL CD147Rg was immobilized on a microtiter plate and incubated overnight at 4 °C in a moist chamber. The other steps were performed at ambient temperature in a moist chamber. Non-specific protein binding was blocked using 2% skim milk in PBS. Fifty microliters of 1 and 5 μg/mL mouse anti-CD147 mAb (M6-1B9 and M6-1E9) were added and incubated for 1 h. The microtiter plate was washed three times with 0.05% Tween20 in PBS and 50 μL of 10 μg/mL purified HuScFvM61B9 was added to the well. After 1 h of incubation, the microtiter plate was washed three times with 0.05% Tween20 in PBS. HRP-conjugated anti-His-tag mAb (BioLegend, 652504) at 1:5000 dilution was subsequently added to the well and incubated for 1 h. TMB substrate was then added to develop the reaction. The absorbance at 450 nm was measured using a microplate reader after adding 1N HCl.

Immunofluorescence analysis of the reactivity of HuScFvM61B9 to CD147 on SupT1 cells

Flow cytometric analysis was performed to evaluate the functional reactivity of HuScFvM61B9 against CD147 on a human T-cell lymphoblastic lymphoma cell line, SupT1, as compared to its parental M6-1B9 mAb[14]. SupT1 cells were washed three times with a FACS buffer and adjusted to 10^7 cells/mL with 10% human AB serum for 30 min on ice to block the Fc receptor. Fifty microliters of 10 μg/mL HuScFvM61B9 was added into 50 μL of blocked cells and incubated on ice for 30 min. The cells were washed twice

with 1% FBS in PBS. After washing, a PE-conjugated anti-His-tag antibody (BioLegend, 362603) at 1:20 dilution was added and incubated on ice for another 30 min. Finally, the cells were washed three times and fixed with 1% paraformaldehyde in PBS. The fluorescence intensity of the stained cells was analyzed using a BD FACSCelesta™ instrument and FlowJo® software.

References

1. Weidle, U. H., Scheuer, W., Eggle, D., Klostermann, S. & Stockinger, H. Cancer-related issues of CD147. *Cancer Genomics Proteomics* **7**, 157-169 (2010).
2. Jia, L., Wang, H., Qu, S., Miao, X. & Zhang, J. CD147 regulates vascular endothelial growth factor-A expression, tumorigenicity, and chemosensitivity to curcumin in hepatocellular carcinoma. *IUBMB Life* **60**, 57-63, doi:10.1002/iub.11 (2008).
3. Nabeshima, K. *et al.* Emmprin (basigin/CD147): matrix metalloproteinase modulator and multifunctional cell recognition molecule that plays a critical role in cancer progression. *Pathol Int* **56**, 359-367, doi:10.1111/j.1440-1827.2006.01972.x (2006).
4. Cui, H. Y. *et al.* Dimerization is essential for HAb18G/CD147 promoting tumor invasion via MAPK pathway. *Biochem Biophys Res Commun* **419**, 517-522, doi:10.1016/j.bbrc.2012.02.049 (2012).
5. He, B. *et al.* Epitope mapping of metuximab on CD147 using phage display and molecular docking. *Comput Math Methods Med*, 1-6, doi:10.1155/2013/983829 (2013).
6. Ku, X. M. *et al.* Epitope mapping of series of monoclonal antibodies against the hepatocellular carcinoma-associated antigen HAb18G/CD147. *Scand J Immunol* **65**, 435-443, doi:10.1111/j.1365-3083.2007.01930.x (2007).

7. Xu, J. *et al.* A randomized controlled trial of Licartin for preventing hepatoma recurrence after liver transplantation. *Hepatology* **45**, 269-276, doi:10.1002/hep.21465 (2007).
8. Chen, Z. N. *et al.* Targeting radioimmunotherapy of hepatocellular carcinoma with iodine (131I) metuximab injection: clinical phase I/II trials. *Int J Radiat Oncol Biol Phys* **65**, 435-444, doi:10.1016/j.ijrobp.2005.12.034 (2006).
9. Bian, H. *et al.* Randomized trial of [131I] metuximab in treatment of hepatocellular carcinoma after percutaneous radiofrequency ablation. *J Natl Cancer Inst* **106**, doi:10.1093/jnci/dju239 (2014).
10. Zhu, H. *et al.* A novel antibody fragment targeting HAb18G/CD147 with cytotoxicity and decreased immunogenicity. *Cancer Biol Ther* **8**, 1035-1044, doi:10.4161/cbt.8.11.8531 (2009).
11. Zhang, Z. *et al.* Preclinical pharmacokinetics, tolerability, and pharmacodynamics of metuzumab, a novel CD147 human-mouse chimeric and glycoengineered antibody. *Mol Cancer Ther* **14**, 162-173, doi:10.1158/1535-7163.MCT-14-0104 (2015).
12. Feng, F. *et al.* Metuzumab enhanced chemosensitivity and apoptosis in non-small cell lung carcinoma. *Cancer Biol Ther* **18**, 51-62, doi:10.1080/15384047.2016.1276126 (2017).
13. Wang, M. *et al.* Dual effects of an anti-CD147 antibody for Esophageal cancer therapy. *Cancer Biol Ther* **20**, 1443-1452, doi:10.1080/15384047.2019.1647052 (2019).
14. Kasinrerk, W., Tokrasinwit, N. & Phunpae, P. CD147 monoclonal antibodies induce homotypic cell aggregation of monocytic cell line U937 via LFA-1/ICAM-

1 pathway. *Immunology* **96**, 184-192, doi:10.1046/j.1365-2567.1999.00653.x (1999).

15. Chiampanichayakul, S., Peng-in, P., Khunkaewla, P., Stockinger, H. & Kasinrerk, W. CD147 contains different bioactive epitopes involving the regulation of cell adhesion and lymphocyte activation. *Immunobiology* **211**, 167-178, doi:10.1016/j.imbio.2005.08.007 (2006).
16. Tragoolpua, K. *et al.* Generation of functional scFv intrabody to abate the expression of CD147 surface molecule of 293A cells. *BMC Biotechnol* **8**, 5, doi:10.1186/1472-6750-8-5 (2008).
17. Intasai, N. *et al.* Potent inhibition of OKT3-induced T cell proliferation and suppression of CD147 cell surface expression in HeLa cells by scFv-M6-1B9. *Immunobiology* **214**, 410-421, doi:10.1016/j.imbio.2008.12.006 (2008).
18. Sangboonruang, S. *et al.* EMMPRIN reduction via scFv-M6-1B9 intrabody affects alpha3beta1-integrin and MCT1 functions and results in suppression of progressive phenotype in the colorectal cancer cell line Caco-2. *Cancer Gene Ther* **21**, 246-255, doi:10.1038/cgt.2014.24 (2014).
19. Thammasit, P. *et al.* Intracellular Acidosis Promotes Mitochondrial Apoptosis Pathway: Role of EMMPRIN Down-regulation via Specific Single-chain Fv Intrabody. *J Cancer* **6**, 276-286, doi:10.7150/jca.10879 (2015).
20. Panich, T., Tragoolpua, K., Pata, S., Tayapiwatana, C. & Intasai, N. Downregulation of Extracellular Matrix Metalloproteinase Inducer by scFv-M6-1B9 Intrabody Suppresses Cervical Cancer Invasion Through Inhibition of Urokinase-Type Plasminogen Activator. *Cancer Biother Radiopharm* **32**, 1-8, doi:10.1089/cbr.2016.2126 (2017).

21. Panich T, M. P., Pata S, Tragoolpua K, Tayapiwatana C, Intasai N. CD147 scFv intrabody-mediated CD147 knockdown inhibits proliferation of human cervical cancer HeLa cells. *Bull Chiang Mai Assoc Med Sci* **47**, 7 (2014).
22. Lopes dos Santos M, Q. W., Manieri TM, Tsuruta LR, Moro AM. . Advances and challenges in therapeutic monoclonal antibodies drug development. *Brazilian Journal of Pharmaceutical Sciences* **54**, e01007 (2018).
23. Kunik, V., Peters, B. & Ofran, Y. Structural consensus among antibodies defines the antigen binding site. *PLoS Comput Biol* **8**, e1002388, doi:10.1371/journal.pcbi.1002388 (2012).
24. Gao, S. H., Huang, K., Tu, H. & Adler, A. S. Monoclonal antibody humanness score and its applications. *BMC Biotechnol* **13**, 55, doi:10.1186/1472-6750-13-55 (2013).
25. Ye, J., Ma, N., Madden, T. L. & Ostell, J. M. IgBLAST: an immunoglobulin variable domain sequence analysis tool. *Nucleic Acids Res* **41**, W34-40, doi:10.1093/nar/gkt382 (2013).
26. Lee, D., Redfern, O. & Orengo, C. Predicting protein function from sequence and structure. *Nat Rev Mol Cell Biol* **8**, 995-1005, doi:10.1038/nrm2281 (2007).
27. Pan, A. C. *et al.* Atomic-level characterization of protein-protein association. *Proc Natl Acad Sci U S A* **116**, 4244-4249, doi:10.1073/pnas.1815431116 (2019).
28. Kozakov, D. *et al.* The ClusPro web server for protein-protein docking. *Nat Protoc* **12**, 255-278, doi:10.1038/nprot.2016.169 (2017).
29. Wisitponchai, T., Shoombuatong, W., Lee, V. S., Kitidee, K. & Tayapiwatana, C. AnkPlex: algorithmic structure for refinement of near-native ankyrin-protein docking. *BMC Bioinformatics* **18**, 220, doi:10.1186/s12859-017-1628-6 (2017).

30. Zhu, K. *et al.* Antibody structure determination using a combination of homology modeling, energy-based refinement, and loop prediction. *Proteins* **82**, 1646-1655, doi:10.1002/prot.24551 (2014).
31. Xue, L. C., Rodrigues, J. P., Kastritis, P. L., Bonvin, A. M. & Vangone, A. PRODIGY: a web server for predicting the binding affinity of protein-protein complexes. *Bioinformatics* **32**, 3676-3678, doi:10.1093/bioinformatics/btw514 (2016).
32. Srila, W. & Yamabhai, M. Identification of amino acid residues responsible for the binding to anti-FLAG™ M2 antibody using a phage display combinatorial peptide library. *Appl Biochem Biotechnol* **171**, 583-589, doi:10.1007/s12010-013-0326-8 (2013).
33. Geysen, H. M. & Mason, T. J. Screening chemically synthesized peptide libraries for biologically-relevant molecules. *Bioorganic Med. Chem. Lett.* **3**, 397-404, doi: 10.1016/S0960-894X(01)80221-3 (1993).
34. Ricatti, J. *et al.* Effects of point mutations in the binding pocket of the mouse major urinary protein MUP20 on ligand affinity and specificity. *Sci Rep* **9**, 300, doi:10.1038/s41598-018-36391-3 (2019).
35. Shawon J, K. A., Shahriar I, Halim MA. Improving the binding affinity and interaction of 5-Pentyl-2-Phenoxyphenol against Mycobacterium Enoyl ACP reductase by computational approach. *Informatics in Medicine Unlocked* **23**, 100528, doi:10.1016/j.imu.2021.100528 (2021).
36. Tayapiwatana, C., Arooncharus, P. & Kasinrerk, W. Displaying and epitope mapping of CD147 on VCSM13 phages: influence of Escherichia coli strains. *J Immunol Methods* **281**, 177-185, doi:10.1016/s0022-1759(03)00270-9 (2003).

37. Akbari, V., Chou, C. P. & Abedi, D. New insights into affinity proteins for HER2-targeted therapy: Beyond trastuzumab. *Biochim Biophys Acta Rev Cancer* **1874**, 188448, doi:10.1016/j.bbcan.2020.188448 (2020).
38. Adolf-Bryfogle, J., Xu, Q., North, B., Lehmann, A. & Dunbrack, R. L., Jr. PyIgClassify: a database of antibody CDR structural classifications. *Nucleic Acids Res* **43**, D432-438, doi:10.1093/nar/gku1106 (2015).
39. Kay, B. K., Kasanov, J. & Yamabhai, M. Screening Phage-Displayed Combinatorial Peptide Libraries. *Methods* **24**, 240-246 (2001).
40. Khoushab, F., Jaruseranee, N., Tanthanuch, W. & Yamabhai, M. Formation of chitin-based nanomaterials using a chitin-binding peptide selected by phage-display. *Int J Biol Macromol* **50**, 1267-1274, doi:S0141-8130(12)00113-4 [pii], doi:10.1016/j.ijbiomac.2012.03.016 [doi] (2012).
41. Koch, C. *et al.* T cell activation-associated epitopes of CD147 in regulation of the T cell response, and their definition by antibody affinity and antigen density. *Int Immunol* **11**, 777-786, doi:10.1093/intimm/11.5.777 (1999).

Author contributions

N.I. performed the experiments and writing the main manuscript text. K.R. performed the epitope mapping experiment. M.Y. gave advice on the epitope mapping experiment. T.P., S.S., W.T., U.Y., K.C. and N.T. performed the experiments. P.N. performed the molecular model and analysis the structure of HuScFvM61B9. C.T. designed humanization process and supervised this study. All authors reviewed the manuscript.

Competing interests

The authors declare no competing interests.